Studies of decoherence in strongly anisotropic spin triangles with toroidal or general non-collinear easy axes

Kilian Irländer[1, *] and Jürgen Schnack[1, †]

[1]*Fakultät für Physik, Universität Bielefeld, Postfach 100131, D-33501 Bielefeld, Germany*
(Dated: January 31, 2023)

Magnetic molecules are investigated with respect to their usability as units in future quantum devices. In view of quantum computing, a necessary prerequisite is a long coherence time of superpositions of low-lying levels. In this article, we investigate by means of numerical simulations whether a toroidal structure of single-ion easy anisotropy axes is advantageous as often conjectured. Our results demonstrate that there is no general advantage of toroidal magnetic molecules, but that arrangements of tilted anisotropy axes perform best in many cases.

I. INTRODUCTION

Molecular spins are being investigated as one prospective platform for quantum computation [1–15]. In order to reduce decoherence effects, clock transitions have been established as promising processes with long lasting coherence [6, 16–19]. Clock transitions are spin transitions made up of two eigenstates having close to the same expectation value of the magnetic moment and thus the same slope of their Zeeman energies as function of applied field. The energy difference which provides the frequency of the transition is thus rather stable against field fluctuations. One preferred constellation is to have zero slope of the Zeeman levels at all, either at the extreme points of Zeeman curves of parabolic shape [6] or for Zeeman curves that belong to zero moments and are thus totally flat [20, 21].

Somewhat along these lines, toroidal magnetic states of molecular nanomagnets [22–41] are considered to be promising candidates of quantum computation since they do not possess magnetic moments for ideally symmetric cases [42]. Several recent publications echo this hypothesis, e.g., [34, 43, 44], however, to our knowledge no decoherence calculations or systematical experiments have actually been performed for such systems. The argument that toroidal quantum states are promising for quantum computing rests on the – maybe reasonable – assumption that they as well are insensitive to weak fluctuating homogeneous magnetic fields [43, 45]. It was, however, shown in e.g. [20, 46] that a true many-body treatment of the interacting system and bath spins goes beyond the mean-field picture of a fluctuating field and that the reason for decoherence is entanglement between system and bath.

In the following we are going to investigate a spin triangle as a typical representative of toroidal magnetic molecules [42]. We study its decoherence while immersed in a bath of nearby spins with mutual dipolar interactions between system and bath spins and among bath

spins. The time evolution of the combined systems is described by the time-dependent Schrödinger equation and thus unitary as in [20]. We thus refrain from mean field assumptions or assumptions about transition matrix elements necessary for a description in terms of Lindblad master equations or perturbation/scattering theory [47, 48]. The Hamiltonian is designed to model the impact of either electronic or nuclear bath spins since nuclear spins are often the source of decoherence in molecular insulators [19, 49–51] whereas electronic spins are the source of decoherence for molecules deposited on metallic surfaces, see e.g. [20, 21]. No approximations as in e.g. [50–52] are made concerning the dipolar interaction; it is fully anisotropic.
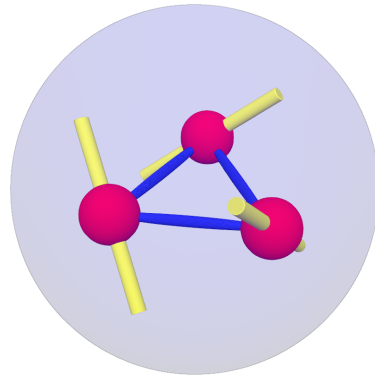

Figure 1. System of three spin-1 particles in red, Heisenberg coupling in blue and anisotropy axes tilted by $\theta_1 = \theta_2 = \theta_3 = \theta$ (here: $\theta = 50°$) in yellow with a varying number of bath spins n_{bath} (chosen between 4 and 10 in this paper) located on the surface of the surrounding purple sphere. Bath spins are coupled to each other and to the system spins via dipole-dipole interactions.

We decided to choose electronic bath spins since the sole purpose of our study, which hopefully initiates further investigations, is to demonstrate that there is no simple correlation between toroidicity and extended coherence times. To this end, we provide examples and systematic studies for numerous arrangements of the surrounding bath of decohering spins. In contrast to widespread

expectations it turns out that a tilted toroidal arrangement of easy anisotropy axes as displayed in Fig. 1 yields the longest coherence times in most of our simulations except for some cases with rather weak anisotropy discussed in Sec. V as well as in the appendix.

The paper is organized as follows. In Sec. II we introduce the employed spin Hamiltonian as well as the necessary technicalities. Section III presents numerical examples whereas Sec. IV, V, VI, and VII, discuss dependencies of coherence times on parameters of the spin system systematically. A summary is given in Sec. VIII.

II. METHODS

We calculate decoherence times of superpositions in a strongly anisotropic triangle of three spins $s = 1$ with easy-axis anisotropy coupled to a spin bath using exact diagonalization and unitary time evolution. To see if there is anything inherently beneficial about toroidal (superposition) states that makes them more stable towards external perturbations in the context of decoherence, we evaluate for which Hamiltonians there are superpositions among the low-lying spectrum with longer or shorter coherence times.

The system considered is displayed in Fig. 1. The three system spins ($s = 1$) are antiferromagnetically coupled and there is a tangential easy-axis anisotropy on each site, i.e. the anisotropy axes are perpendicular to the altitude of the equilateral triangle formed by the sites of these three system spins reminiscent of e.g. Dy$_3$ toroidal molecules [22, 42]. We consider a bath of ($s = \frac{1}{2}$) spins that are coupled to each other and to the system spins via dipole-dipole interactions. The number of bath spins is chosen between 4 and 10. This small number is sufficient for our purpose. The system spins are located at a distance of $r_s = 1$ from the origin, while bath spins are placed randomly on the sphere around the origin with radius $r_b = 2$ (in arbitrary units, see below).

The complete Hamiltonian

$$\underset{\sim}{H} = \underset{\sim}{H}_\text{S} + \underset{\sim}{H}_\text{SB} + \underset{\sim}{H}_\text{B} \tag{1}$$

is made up of the system Hamiltonian $\underset{\sim}{H}_\text{S}$, the system-bath interaction Hamiltonian $\underset{\sim}{H}_\text{SB}$ and the bath-bath interaction Hamiltonian $\underset{\sim}{H}_\text{B}$. The system Hamiltonian $\underset{\sim}{H}_\text{S}$ is comprised of three terms, the Heisenberg exchange interaction

$$\underset{\sim}{H}_\text{Heisenberg} = -2J \cdot \sum_{i=0}^{2} \vec{\underset{\sim}{s}}_i \cdot \vec{\underset{\sim}{s}}_{i+1} \tag{2}$$

with $\vec{\underset{\sim}{s}}_3 \equiv \vec{\underset{\sim}{s}}_0$, the single-spin (single-ion) anisotropy

$$\underset{\sim}{H}_\text{anisotropy} = \sum_{i=0}^{2} \vec{\underset{\sim}{s}}_i \cdot \mathbf{D} \cdot \vec{\underset{\sim}{s}}_i \tag{3}$$

with the anisotropy tensors $\mathbf{D}_i$ as well as a Zeeman interaction term. All calculations were performed with a weak magnetic field $B_z = 0.05$ T acting only on the central spin system. This splits the states that are degenerate at $B = 0$ in order to be able to distinguish them numerically. We have numerically verified that while there is some quantitative effect on coherence times there is no significant qualitative difference to the situation with $B = 0$.

The system-bath Hamiltonian $\underset{\sim}{H}_\text{SB}$ is defined as follows

$$\underset{\sim}{H}_\text{SB} = \sum_{\substack{i=0, \\ j=3}}^{2,N} \frac{A_1}{r_{ij}^3} \left(\vec{\underset{\sim}{s}}_i \cdot \vec{\underset{\sim}{s}}_j - \frac{3 \left(\vec{\underset{\sim}{s}}_i \cdot \vec{r}_{ij} \right) \left(\vec{\underset{\sim}{s}}_j \cdot \vec{r}_{ij} \right)}{r_{ij}^2} \right) \tag{4}$$

with

$$A_1 = \frac{\mu_0 g_\text{S} \mu_\text{S} g\mu}{4\pi} . \tag{5}$$

The bath Hamiltonian $\underset{\sim}{H}_\text{B}$ reads

$$\underset{\sim}{H}_\text{B} = \sum_{3 \leq i < j}^{N} \frac{A_2}{r_{ij}^3} \left(\vec{\underset{\sim}{s}}_i \cdot \vec{\underset{\sim}{s}}_j - \frac{3 \left(\vec{\underset{\sim}{s}}_i \cdot \vec{r}_{ij} \right) \left(\vec{\underset{\sim}{s}}_j \cdot \vec{r}_{ij} \right)}{r_{ij}^2} \right) \tag{6}$$

with

$$A_2 = \frac{\mu_0 (g\mu)^2}{4\pi} . \tag{7}$$

Here μ_0 is the vacuum permeability while $g\mu$ and $g_\text{S}\mu_\text{S}$ denote the magnetic interaction strength of the bath and system spins, respectively. We do not specify them, and we do not specify the unit of length since we take A_1 and A_2 as adjustable parameters of our investigation that would enable us to switch between electronic and nuclear bath spins. We would like to emphasize that we do not approximate the dipolar interactions by their diagonal, i.e. Heisenberg-like part, as often done, see e.g. [50–52] as typical examples. If the dipolar interaction is approximated by terms of the form $2\underset{\sim}{s}_i^z \underset{\sim}{s}_j^z + \underset{\sim}{s}_i^x \underset{\sim}{s}_j^x + \underset{\sim}{s}_i^y \underset{\sim}{s}_j^y$, then total $\underset{\sim}{S}^z$ is a conserved quantity for this interaction as it is for the Heisenberg part of the Hamiltonian. We are truly convinced that the symmetry-breaking anisotropic parts of the dipolar interaction play an important role for decoherence since they allow many more transitions like for instance flip-flop transitions which are often discussed in a perturbation picture of decoherence, compare e.g. [16].

In Ref. [20], the effects of the magnitude of system parameters A_1 and A_2 are illustrated. To summarize, A_1 has a significant effect on the time scale of decoherence for all superpositions. This is because the many-body energy eigenstates of the full system get less and less energetically isolated as A_1 is increased and the original Zeeman structure of the system is lost when adding the bath and considering the full system. A_2 controls the

relative differences in coherence times between different superpositions but affects them a lot less than A_1. In an approximate mean-field picture a strong A_1 would lead to stronger time-dependent detunings of the effective magnetic field at the site of the system spins, thus destroying the coherence of the transition. Our findings align with these general statements, and A_1 and A_2 are chosen to have fixed values of 0.1 K for all following calculations (for other values of A_1 and A_2 see the Appendix). This somewhat arbitrary choice is justified as the aim of these investigations is to find relative differences in coherence times, not calculating them accurately for realistic systems.

The decoherence times are calculated via time evolution based on exact diagonalization. To perform the time evolution of the whole system with a time-independent magnetic field, let $\{|a_i\rangle\}$ be the eigenbasis of the initial ($t = 0$) Hamiltonian of the system A. Initialize A into an initial state $|\Psi_A(t=0)\rangle$. Most often, this will be a superposition of two non-degenerate states n and p

$$|\Psi_A(t=0)\rangle = \frac{1}{\sqrt{2}}\left(|a_n\rangle + |a_p\rangle\right) . \tag{8}$$

Then define a random initial state $|\Psi_B(t=0)\rangle$ for the bath B and form a product state

$$|\Psi_0\rangle = |\Psi(t=0)\rangle = |\Psi_A(t=0)\rangle \otimes |\Psi_B(t=0)\rangle . \tag{9}$$

Let $\{|m\rangle\}$ be the product basis of the whole system $(A \otimes B)$ and $\{|\varphi_l\rangle\}$ the eigenbasis of the Hamiltonian of the whole system with eigenvalues E_l. Then a change into this eigenbasis

$$|\Psi_0\rangle = \sum_{l=1}^{\dim(\mathrm{H})} \langle\varphi_l|\Psi_0\rangle \cdot |\varphi_l\rangle \tag{10}$$

yields for the time-evolved state

$$|\Psi(t)\rangle = \sum_{l=1}^{\dim(\mathrm{H})} e^{i \cdot E_l \cdot t} \langle\varphi_l|\Psi_0\rangle \cdot |\varphi_l\rangle . \tag{11}$$

Changing back into the product basis gives

$$|\Psi(t)\rangle = \sum_{l,m=1}^{\dim(\mathrm{H})} e^{i \cdot E_l \cdot t} \langle\varphi_l|\Psi_0\rangle \cdot \langle m|\varphi_l\rangle \cdot |m\rangle . \tag{12}$$

All terms in this equation are known to machine precision by exact diagonalization.

In order to quantify the decoherence of the superposition, we employ the reduced density matrix, denoted by ρ, as a quantifier. There are various options for the quantification of decoherence but in our context it does not really matter which one is chosen, and we just consider the absolute value of the off-diagonal element of ρ. If the initial state was a superposition as defined in Eq. (8), this quantity can simply be calculated as

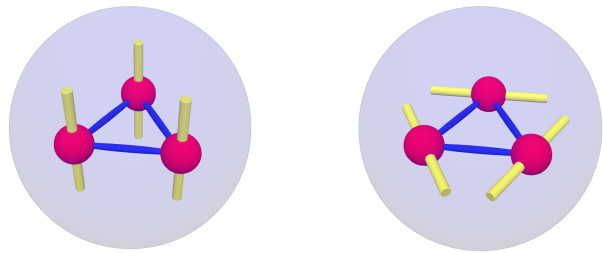$$|\rho_{n,p}| = |\langle a_n|\underset{\sim}{\rho}|a_p\rangle| . \tag{13}$$

Figure 2. LHS: System for $\theta = 0°$; this would be a typical SMM configuration. RHS: System for $\theta = 90°$; this corresponds to a perfect toroidal configuration. For angles inbetween see Fig. 1.

In this paper we investigate the dependence of decoherence rates on the tilting of all anisotropy axes along the global θ direction where $\theta = 0°$ corresponds to a perfect alignment of easy anisotropy axes for a single molecule magnet (SMM) and $\theta = 90°$ represents a perfect toroidal configuration, see Fig. 2. The configuration with $\theta = 90°$ will however not be considered in this paper as it is then impossible to initialize a toroidal moment with a magnetic field in z-direction because the field direction is perpendicular to the one of the easy axes. We will also need a definition of the toroidal magnetic moment of a spin triangle in order to evaluate its relevance for decoherence rates. This is given by

$$\underset{\sim}{\vec{\tau}} = g \cdot \mu_B \sum_{i=0}^{2} \vec{r}_i \times \underset{\sim}{\vec{s}}_i , \tag{14}$$

with $\vec{r}_i$ being the classical positions of the spins contributing to the sum. Then τ_z, as used in later figures, is defined as the expectation value with respect to the initial state, compare (9),

$$\tau_z = \langle\Psi_A(t=0)|\underset{\sim}{\tau}_z|\Psi_A(t=0)\rangle . \tag{15}$$

III. EXAMPLES OF DECOHERENCE CALCULATIONS

To model a strongly anisotropic system, $J = -10$ K and $D = -50$ K are chosen in order to work with (order of magnitude) typical numbers. A few examples using different parameters are provided in the appendix. Some of the resulting Zeeman diagrams as a function of B_z displaying the lowest eight eigenstates are shown in Fig. 3.
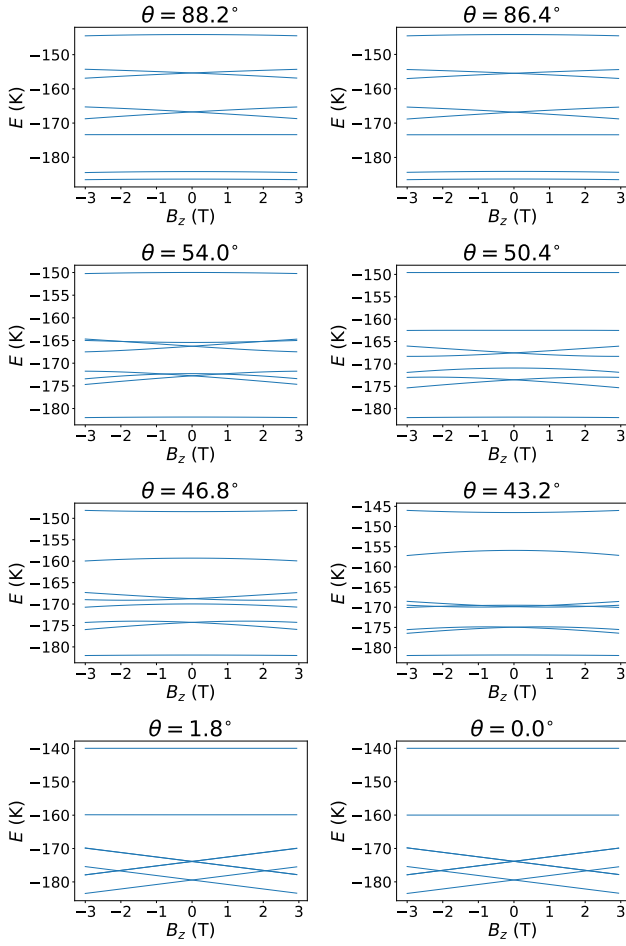
Figure 3. Zeeman diagrams of the eight lowest-lying states of the system without bath for different values for the tilting angle of the anisotropy axes θ. For a given B_z (typically $B_z = 0.05$ T) the states are enumerated $0, 1, 2, 3, \ldots$ from below.

In order to test which system configurations and which superpositions show the longest coherence times, we consider all possible two-state superpositions of the six energetically lowest eigenstates for different values of θ at $B_z = 0.05$ T and perform a time evolution as laid out above. We ignore possible experimental difficulties concerning the initialization of these superpositions [53] as we aim to identify characteristics of those superpositions which display long coherence times. In order to avoid duplicate plot legends, the color code for the superpositions is displayed once in Fig. 4.

Some sample results corresponding to the Zeeman diagrams from Fig. 3 are shown in Fig. 5. While many superpositions decohere almost instantly, others show significantly longer coherence times. In the SMM configuration ($\theta = 0°$), all superpositions decohere quickly, while for the almost toroidal configuration ($\theta = 88.2°$), there are some states which survive a decent amount of time. For the parameter configuration chosen here, however, middle-sized angles $\theta \approx 50°$ perform best in most cases.
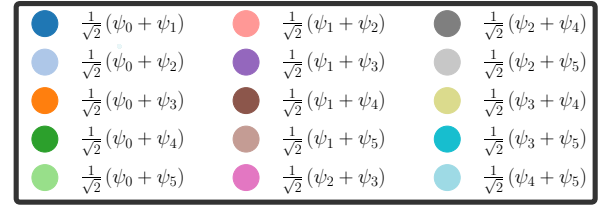

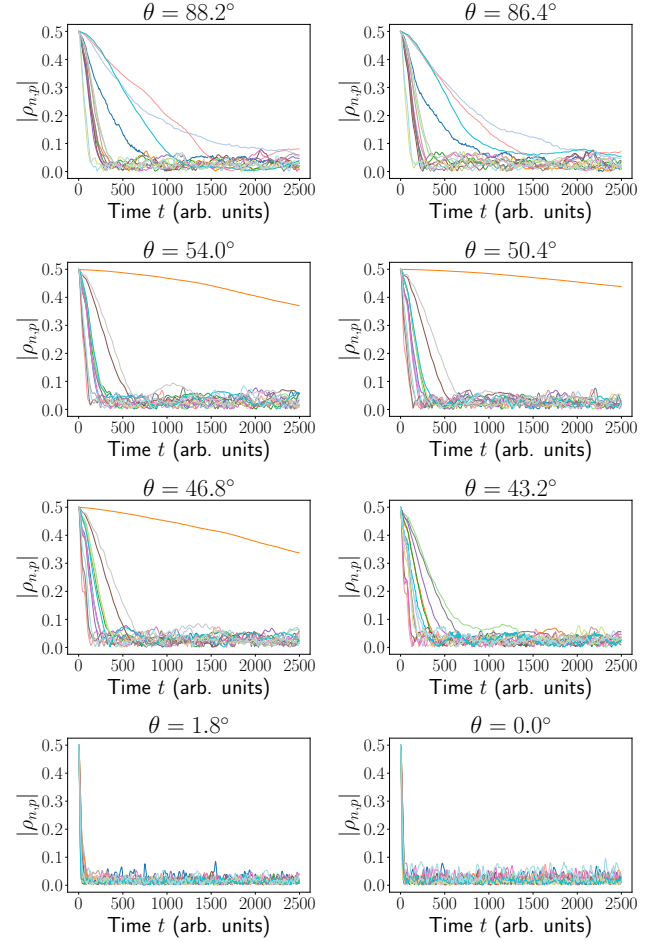Figure 4. Legend to show which superposition is represented by which color.

Figure 5. Decoherence (see Eq. (13)) over time of all two-state superpositions of the six lowest-lying energy eigenstates for a fixed random bath with $n_{\text{bath}} = 8$; angles θ correspond to Fig. 3. Legend is displayed in Fig. 4.

To make system configurations and superpositions comparable, we choose to consider the time it takes for the absolute value of the off-diagonal element to fall below the more or less arbitrarily chosen value of 0.49 for the first time for a given superposition. This time is denoted by $T_{0.49}$. In Fig. 6, we first verify the claim that superpositions of states with near-identical magnetic moments (clock transitions) indeed survive the longest. To this end, we calculate the absolute value of the difference in the magnetic moment M_ν for each superposition and

compare it to the corresponding coherence time. Here, the magnetic moment of a state is defined as the negative expectation value of the $\underset{\sim}{S}_z$ operator acting on the system without bath times the gyromagnetic factor $g = 2$ times the Bohr magneton μ_B. Figure 6 (top) shows that only states with small differences in magnetic moment can form superpositions expressing long coherence times. However, this property of clock transitions is not sufficient to predict well-performing superpositions as can be deduced from Fig. 6 (bottom). There must be additional factors at play in order to explain why some superpositions perform poorly despite $|M_p - M_n|$ being very small.
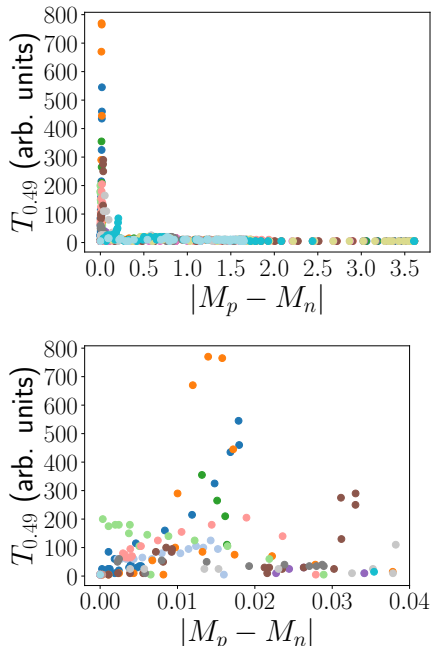
Figure 6. Coherence times vs. the absolute value of the difference in the expectation value for S_z of the eigenstates in each superposition ($|M_p - M_n|$) for 50 values of θ between 0° and 88.2° at $B_z = 0.05$ T for a random bath with $n_{\text{bath}} = 8$. Top: Only superpositions $|M_p - M_n| \approx 0$ have comparatively long coherence times. Bottom: Zoomed-in view. While $|M_p - M_n| \approx 0$ is necessary, however, it is not sufficient to predict long coherence times. Legend is displayed in Fig. 4.

As a sidenote, we checked that this cannot be explained by the second derivative of the energy difference with respect to the magnetic field either. Rather, it is probably related to the way a certain clock transition couples to the decohering bath.

Figure 7 (top) provides an impression that systems with strong SMM ($\theta \approx 0°$) or toroidal ($\theta \approx 90°$) orientation of the anisotropy axes both do not contain low-lying states to form long-living clock transitions. Rather, mid-sized angles seem to be most promising for the given parameter configuration. This is a strong indication against the simple idea that superpositions with a larger toroidal moment should display longer coherence times. And, *vice versa*, there is also no indication of superpositions
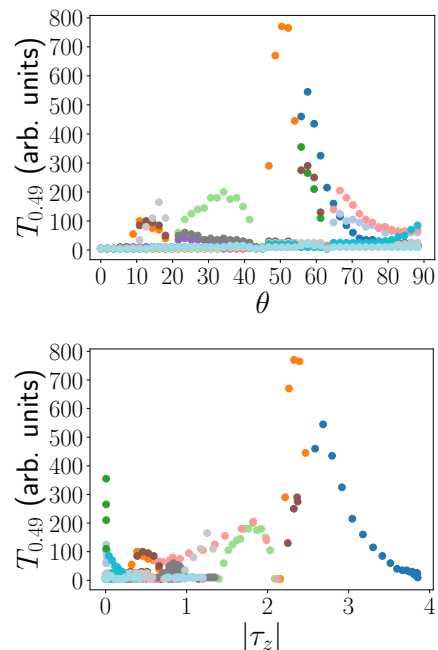

Figure 7. Coherence times vs. tilting angle (top) and absolute value of the z-component of the toroidal moment of superpositions (bottom, see Eq. (14)) for 50 values of θ between 0° and 88.2° at $B_z = 0.05$ T for a random bath with $n_{\text{bath}} = 8$. Best coherence times are observed for mid-sized angles and toroidal moments. Legend is displayed in Fig. 4. There is no one-to-one relation between θ and the expectation value of the toroidal moment; the latter may simply vanish for certain energy eigenstates or their superpositions even if $\theta \neq 0$.

of states forming a clock transition having large toroidal moments which is, although not sufficient on its own, obviously the deciding factor for long coherence times.
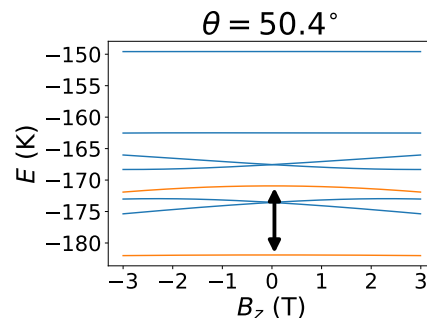

Figure 8. Zeeman diagram of the six lowest-lying states of the system without bath for $\theta = 50.4°$. The black arrow indicates the transition with the longest coherence time (see also Fig. 10) made up of the two orange states.

IV. DEPENDENCE OF COHERENCE TIMES ON THE PLACEMENT AND NUMBER OF BATH SPINS

The best performing superposition of the system with the parameters introduced above is found numerically around a tilting angle of $\theta = 50.4°$ for the superposition of the ground state and the third excited state. In the following, we use this as a sample system in order to illustrate our findings.

Note that $\theta = 50.4°$ is not a universal "magic angle" as the performance of superpositions is highly dependent on the parameter configuration and therefore the ideal angle changes when altering the magnitude of parameters such as D and J as will be shown in Sec. V. Figure 8 shows the Zeeman diagram of the system without bath for $\theta = 50.4°$ together with the best-performing transition.
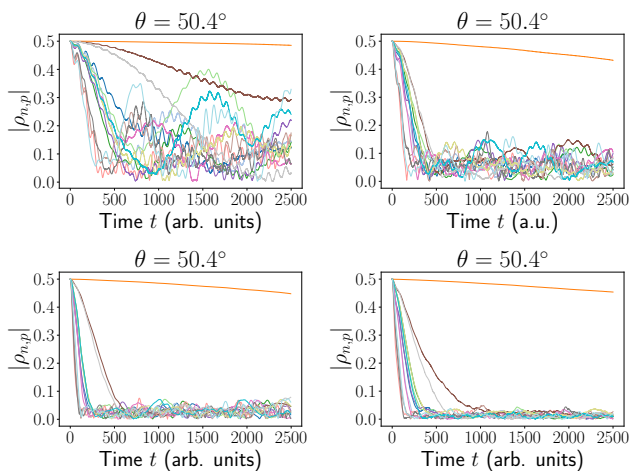

Figure 9. Decoherence over time of all two-state superpositions of the six lowest-lying energy eigenstates for $n_{\text{bath}} = 4$ (top left), $n_{\text{bath}} = 6$ (top right), $n_{\text{bath}} = 8$ (bottom left), $n_{\text{bath}} = 10$ (bottom right), $B_z = 0.05$, and $\theta = 50.4°$. Legend is displayed in Fig. 4.

In order to evaluate the effect of changes of the spin bath and to eliminate the possibility of accidentally choosing a non-typical bath, the decoherence calculations were repeated for baths with a different number of bath spins, see Fig. 9, as well as for ten different sets of $n_{\text{bath}} = 8$ randomly placed bath spins, see Fig. 10. Both Fig. 9 and Fig. 10 show that while coherence times are somewhat dependent on the nature of the spin bath, the main qualitative findings regarding which superpositions show long coherence times and which do not are largely independent of the number and placement of bath spins. In particular, the robustness of $1/\sqrt{2}(\psi_0 + \psi_3)$ (orange curves) both against various arrangements of the bath spins and various sizes is astonishing as well as encouraging in view of future applications.

We have numerically verified that these results for a tilting angle of $\theta = 50.4°$ are representative for other angles. For simplicity, most of the following calculations
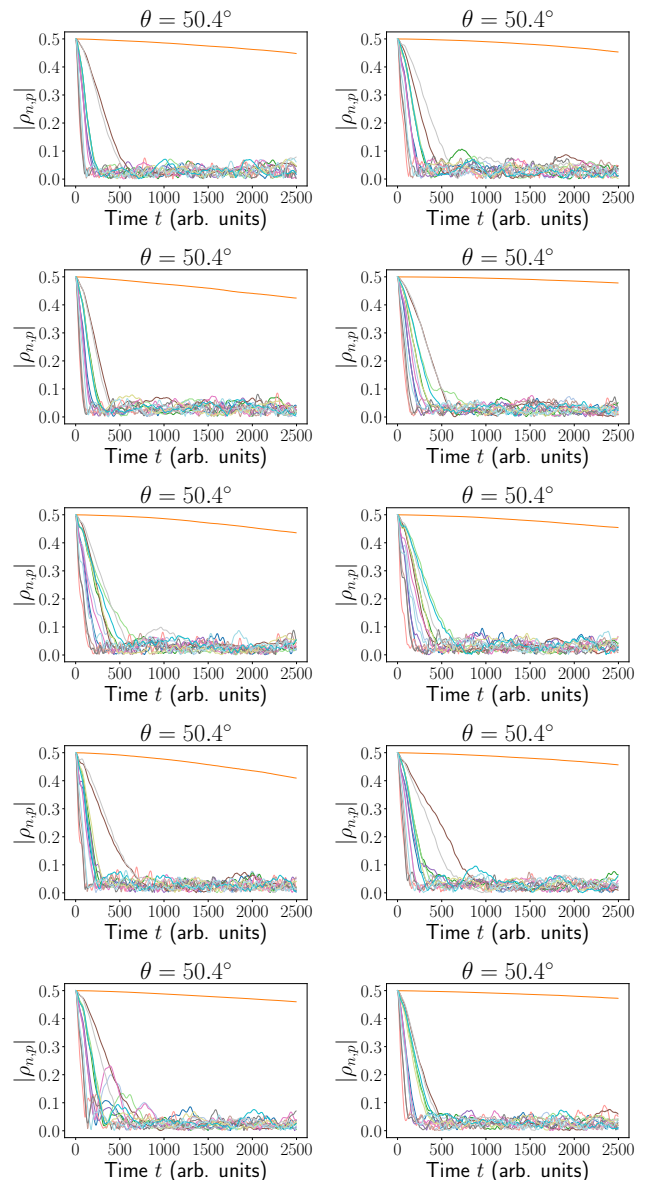

Figure 10. Decoherence over time of all two-state superpositions of the six lowest-lying energy eigenstates for 10 different random baths with $n_{\text{bath}} = 8$ at $B_z = 0.05$ and $\theta = 50.4°$. Legend is displayed in Fig. 4.

have been performed using only a single random bath. This is justified as the concrete values of the coherence times are of no particular relevance to our findings and the relative differences between superpositions are very similar across all random baths we used.

V. DEPENDENCE OF COHERENCE TIMES ON THE MAGNITUDE OF J AND D

In this section, we aim to take a look at if and how the ideal tilting angle of $\theta = 50.4°$ found for the chosen $J = -10$ K and $D = -50$ K changes with J and D.

Figures 11 and 12 show the dependency in regards to J and D, respectively.
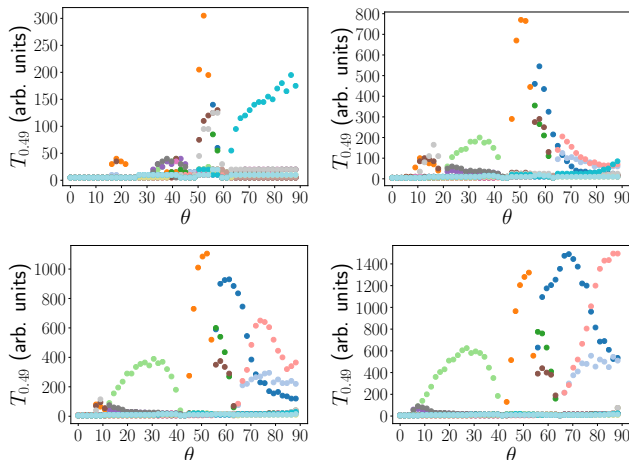

Figure 11. Coherence times vs. tilting angle for $D = -50$ K and (from top to bottom) $J = -5$ K, $J = -10$ K, $J = -15$ K, $J = -20$ K for 50 values of θ between $0°$ and $88.2°$ at $B_z = 0.05$ T for a single bath with $n_{\text{bath}} = 8$. Legend is displayed in Fig. 4.
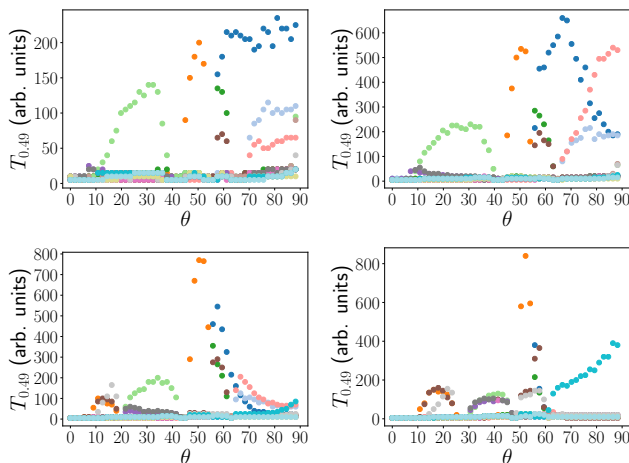

Figure 12. Coherence times vs. tilting angle for $J = -10$ K and (from top to bottom) $D = -10$ K, $D = -25$ K, $D = -50$ K, $D = -100$ K for 50 values of θ between $0°$ and $88.2°$ at $B_z = 0.05$ T for a single bath with $n_{\text{bath}} = 8$. Legend is displayed in Fig. 4.

There are some competing trends in the data but for strongly anisotropic systems, the ideal angle is always at around $50°$ while for systems with weaker anisotropies D (compared to the exchange interaction J), this angle may lie close to $90°$. It should be mentioned here that one would not speak of a toroidal system if the anisotropy was not dominant. These results show the exact opposite of what would be expected if the argument for superpositions with strong toroidal moments having long coherence times was right: The more anisotropic the system,

the more stable the toroidal states should become. In our calculations, the configurations near $\theta = 90°$, which contain superpositions with high toroidal moments, are doing worse in terms of coherence times when the strength of the anisotropy is increased, compare Fig. 12.

VI. GAP SIZES AND COHERENCE TIMES

The size of the energy gap ΔE between the two superposed states is an easily measured characteristic of a clock transition. It is obvious that by scaling up J and D, the spacing of the energy levels and therefore ΔE will increase. It is also obvious that this will lead to longer coherence times when we leave the coupling to the bath A_1 unchanged as this is akin to reducing A_1 while keeping J and D unchanged which is a situation which was already investigated to some extend in see Sec. II and is also covered in the appendix. Therefore one might arrive at the conclusion that large energy gaps ΔE always lead to longer coherence times. To test if this is true, we investigate how coherence times depend on ΔE by changing the tilting angle θ instead of J and D. The clock transition of the two lowest-lying states in the almost "toroidal" flat triangle ($\theta = 88.2°$) configuration is chosen as an example. As θ is decreased, the upper superposition state sometimes changes order with other states as can be inferred from Fig. 13 while the lower state always stays the ground state.
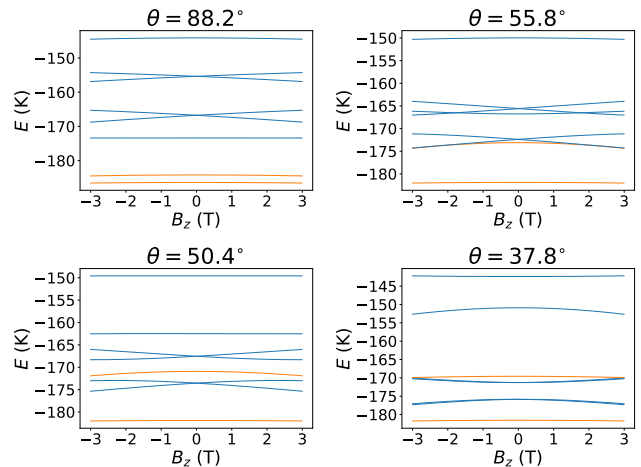

Figure 13. Zeeman diagrams of the eight lowest-lying states of the system without bath for some sample values of θ. The states to be used for decoherence calculations are colored in orange. Notice the different scalings on the y-axes.

The results for the decoherence calculations of these systems are displayed in Fig. 14. Here, the idea is to show decoherence time, gap size and tilting angle all in one figure without having to resort to 3D plots. The colored dots indicate decoherence time vs. gap size while, starting in the left-hand lower corner with $\theta = 88.2°$ (almost toroidal configuration), the red arrows always point

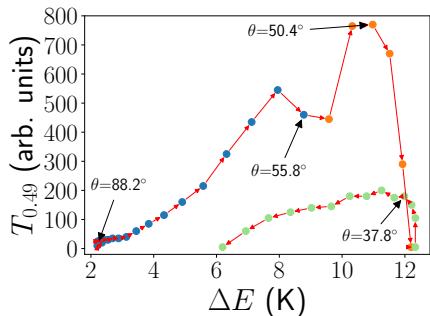to the next configuration with the tilting angle decreased by 1.8°.

Figure 14. Coherence times vs. gap size ΔE for the superposition indicated by the orange states in Fig. 13 for different values of θ for a single bath with $n_{\text{bath}} = 8$. The dots are colored according to the legend displayed in Fig. 4 and indicate the calculated coherence times. Red arrows connect consecutive values of θ; they start in the almost "toroidal" configuration at $\theta = 88.2°$ and always point to the next configuration with θ decreased by 1.8° until $\theta = 19.8°$. Blue arrows indicate data points corresponding to the systems displayed in Fig. 13.

There seems to be a strong positive relationship between gap size and coherence time between $\theta = 88.2°$ and $\theta = 50.4°$ interrupted only by a brief decrease in coherence times between $\theta = 57.6°$ and $\theta = 54°$ as one of the superposition states gets energetically close to other eigenstates with which it can now be connected via interactions with the spin bath and therefore decoheres. In this range of tilting angles, the upper superposition state is either the energetically second or fourth lowest state. When decreasing the tilting angle further, it again gets energetically close to other states which causes the coherence time to collapse almost to zero. From approximately $\theta = 45°$ on, the upper superposition state is now the sixth lowest eigenstate and there is no clear correlation between gap size and coherence times. The reason for this is not well understood and warrants further investigation.

VII. IMPACT OF A SYMMETRY-BREAKING DIPOLAR INTERACTION

As discussed in Ref. [54], a Hamiltonian consisting of a Heisenberg term and single-ion easy anisotropy axes is invariant under a collective rotation of all anisotropy axes (and the field direction) by a common angle. Therefore, a rotation by e.g. $\varphi = -\pi/2$, which rotates all anisotropy axes to point inwards, see Fig. 15, yields the same energy spectrum and leaves (many) observables unchanged. The superpositions, however, have zero toroidal moment now.
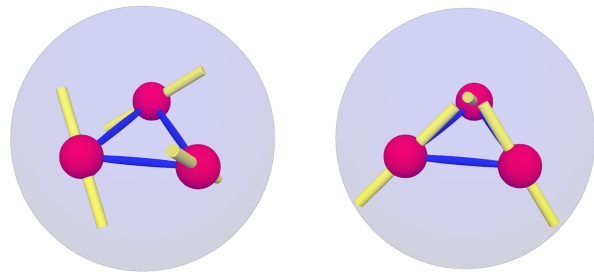

Figure 15. 3D representation of the spin system from Fig. 1 (left) and with anisotropy axes rotated by $\varphi = -\pi/2$ (right).

Out of curiosity, we introduced a symmetry-breaking dipole-dipole interaction between the system spins (we could have also chosen a Dzyaloshinskii-Moriya interaction) to see if there would be any effect on the coherence times if the above mentioned symmetry is lost and the toroidal character of the system even stabilized [54]. The new system Hamiltonian then reads

$$\underset{\sim}{H}_{\text{S}}^{\text{N}} = \underset{\sim}{H}_{\text{Heisenberg}} + \underset{\sim}{H}_{\text{anisotropy}} + \underset{\sim}{H}_{\text{Zeeman}} \tag{16}$$

$$+ \sum_{\substack{i=0, \\ j=i+1}}^{2} \frac{A_3}{r_{ij}^3} \left(\underset{\sim}{\vec{s}}_i \cdot \underset{\sim}{\vec{s}}_j - \frac{3 \left(\underset{\sim}{\vec{s}}_i \cdot \vec{r}_{ij} \right) \left(\underset{\sim}{\vec{s}}_j \cdot \vec{r}_{ij} \right)}{r_{ij}^2} \right)$$

with the third spin being again the zeroth spin so that all system spins are coupled to each other.

When choosing A_3 to be very small, the symmetry is broken but numerically, the difference in coherence times is also very small; the superpositions with large toroidal moments do not perform significantly better than before.
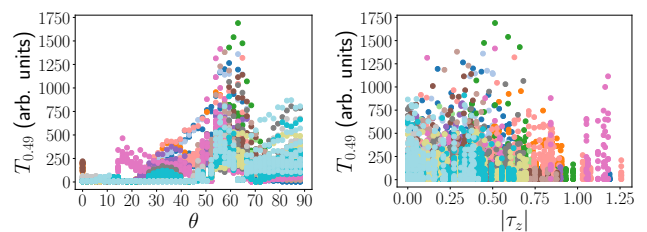

Figure 16. Coherence times vs. tilting angle (left) and absolute value of the z-component of the toroidal moment of superpositions (right, see Eq. (14)) with additional dipole interactions between central spins with $A_3 = |J| = 10$ K for 50 values of θ between $0°$ and $88.2°$ at $B_z = 0.05$ T for ten different random baths with $n_{\text{bath}} = 8$. Again, best coherence times are observed for mid-sized angles and toroidal moments although the latter now have a smaller range compared to the original system, see Fig. 7. Legend is displayed in Fig. 4.

Choosing an A_3 with the same magnitude as J, Fig. 16 shows there are even fewer states with large toroidal moments displaying long coherence times. We repeated the calculation for ten different random baths to again eliminate the possibility of choosing a non-typical bath. Otherwise, there are no significant new findings; the system

behaves very similarly to the one without dipolar interactions between the system spins, see Fig. 7.

VIII. DISCUSSION AND CONCLUSIONS

On the basis of our calculations, we can state that systems with maximally "toroidal"-oriented anisotropy axes do not necessarily exhibit long coherence times. There are a number of factors at play, mainly the need for $|M_p - M_n|$ to be small, while other factors such as the energy gap and perhaps the toroidal moment enter in a complex way and cannot be considered independently of each other. It was shown that, for the example of a spin-1 triangle, superpositions with large toroidal moments can exhibit even very short coherence times. All in all, we found no evidence that toroidicity should be a desirable characteristic when designing, e.g., a qubit with long coherence times. To our surprise, rather, non-collinear tilted anisotropy axes that are almost mutually orthogonal seem to be most promising in many cases. The fundamental advantage of these systems is given by the presence of clock transitions amongst the energetically low-lying states which is a feature not easily inferred from the geometry or other characteristics of the system.

The present paper mainly states numerical findings about decoherence properties of a triangular arrangement of spins with C_3-symmetric anisotropy axes. The very interesting question *why* certain superpositions decohere more slowly and how these effects are influenced by e.g. the size of energy gaps of the system compared to the spectral width of the bath remains open and thus subject to further studies. From previous studies we know that decoherence is intimately related to entanglement between system and bath [20] which suggests that some initial states entangle more easily and quickly than others for a given Hamiltonian of the total system.

Appendix A: Investigations for other parameters of the system

Following a suggestion by a referee, we considered different values for the system-bath coupling strength A_1 and the bath-bath coupling strength A_2 as choosing them to be the same indicates an electronic spin bath which is maybe too special. Furthermore, we also looked at a system with $J = -1$ K and $D = -10$ K to work with
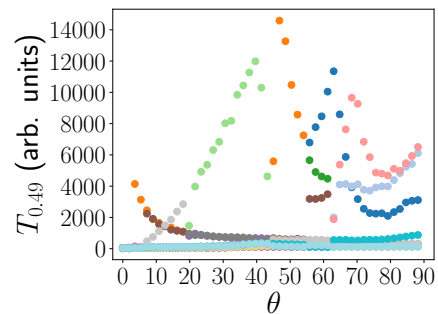

Figure 17. Coherence times vs. tilting angle for 50 values of θ between $0°$ and $88.2°$ at $B_z = 0.05$ T for a random bath with $n_{\text{bath}} = 8$, $A_1 = 0.01$ K, and $A_2 = 0.001$ K. Observations align with those for the system with $A_1 = A_2 = 0.1$ K shown in Fig. 7. Legend is displayed in Fig. 4.
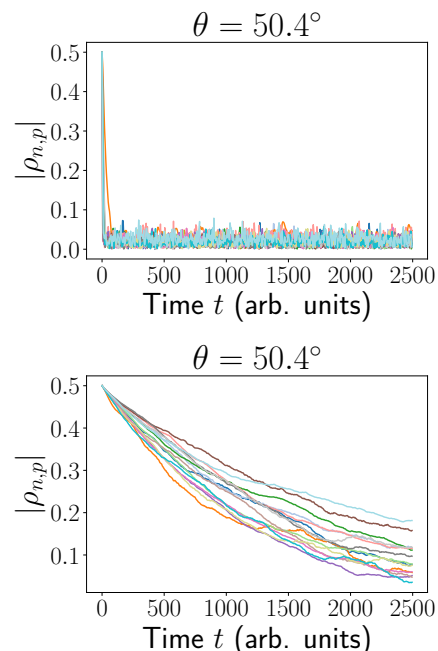

Figure 18. Decoherence over time of all two-state superpositions of the six lowest-lying energy eigenstates for a random bath with $n_{\text{bath}} = 8$ at $B_z = 0.05$ and $\theta = 50.4°$ with $A_1 = 1.0$ K and $A_2 = 0.1$ K (top) or $A_1 = 0.1$ K and $A_2 = 100.0$ K (bottom). At these extremes, all superpositions perform equally well and there are no advantages in coherence times for clock transitions. Large A_1 lead to virtually instantaneous decoherence, while large A_2 lead to neither very quick nor very slow decoherence. Legend is displayed in Fig. 4.

numbers more typical for dysprosium triangles. Our aim here is to show that our main qualitative findings hold for a wide range of parameters.

1. Variation of A_1 and A_2 in the standard system described in the paper

Figure 17 shows the coherence times of all superpositions considered vs. the tilting angle θ for the standard system with $J = -10$ K and $D = -50$ K but with $A_1 = 0.01$ K and $A_2 = 0.001$ K instead of $A_1 = A_2 = 0.1$ K. This could e.g. represent a bath of protons. As expected, the coherence times increase substantially, as the coupling between system and bath is now an order of magnitude weaker. Other than that, however, the findings align with the main qualitative observations of the standard configuration shown in Fig. 7.

This behaviour only breaks down when considering very strong A_1 and/or A_2, see Fig. 18 for an example. If A_1 is chosen too large, no superposition has a significant coherence time and all decohere apparently instantly. We believe that the reason for this behaviour is that the Zeeman levels of the original system entangle strongly with the bath and are thus deformed so extremely that it does not matter if they formed a clock transition in the original system.

If A_2 is chosen very large, all superpositions show similar, mid-sized coherence times. We believe this to be caused by the fact that the states of each superposition can, when combined with the energetically now very broad spectrum of the environment, be energetically connected to a multitude of other states of the original system. On the other hand, the density of bath states is significantly reduced, so that the process of decoherence may be hindered to some extend as suggested in [20].

2. More realistic values of J and D to approximately represent dysprosium triangles

Papers claiming toroidal moments to be promising candidates for quantum technologies often consider triangles of dysprosium [22, 42]. Therefore, we choose $J = -1$ K and $D = -10$ K in order to work with more realistic values for the Heisenberg interaction and strength of the anisotropy. We find, as shown in Fig. 19, that there are again some superpositions with long coherence times

around $\theta = 50°$. However, the best-performing superpositions are made up of the third and fifth excited states similar to those in Fig. 11 (top) and Fig. 12 (bottom). These have almost zero toroidal moment and therefore do not disprove the main statement of this paper.
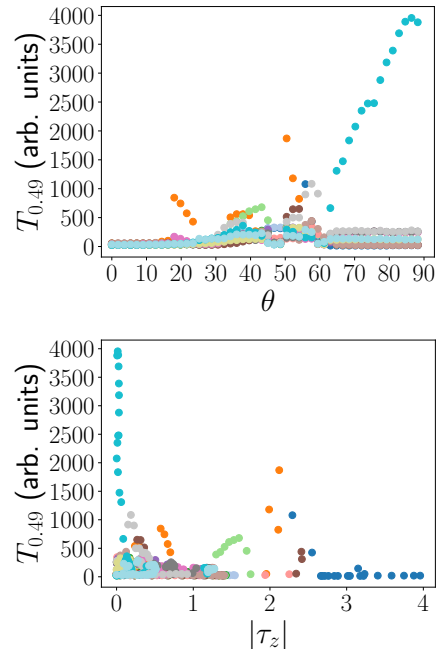

Figure 19. Coherence times vs. tilting angle (top) and absolute value of the z-component of the toroidal moment of superpositions (bottom, see Eq. (14)) for 50 values of θ between $0°$ and $88.2°$ at $B_z = 0.05$ T for a random bath with $n_{bath} = 8$, $J = -1$ K, and $D = -10$ K, $A_1 = 0.01$ K, $A_1 = 0.001$ K. The coherence times are again very similar to those shown for the system with $J = -10$ K, $D = -50$ K, see Fig. 7 with the exception of the superposition of the third and fifth excited states at angles $\theta \gtrsim 60°$. However, these superpositions have a toroidal moment close to zero so that they are of no significance to the main findings of this paper. Legend is displayed in Fig. 4.

[1] A. Morello, P. C. E. Stamp, and I. S. Tupitsyn, Pairwise decoherence in coupled spin qubit networks, Phys. Rev. Lett. **97**, 207206 (2006).

[2] A. Ardavan, O. Rival, J. J. L. Morton, S. J. Blundell, A. M. Tyryshkin, G. A. Timco, and R. E. P. Winpenny, Will spin-relaxation times in molecular magnets permit quantum information processing?, Phys. Rev. Lett. **98**, 057201 (2007).

[3] W. Wernsdorfer, A long-lasting phase, Nature Materials **6**, 174 (2007).

[4] S. Takahashi, I. S. Tupitsyn, J. van Tol, C. C. Beedle, D. N. Hendrickson, and P. C. E. Stamp, Decoherence in crystals of quantum molecular magnets, Nature **476**, 76 (2011).

[5] D. Kaminski, A. L. Webber, C. J. Wedge, J. Liu, G. A. Timco, I. n. J. Vitorica-Yrezabal, E. J. L. McInnes, R. E. P. Winpenny, and A. Ardavan, Quantum spin coherence in halogen-modified Cr$_7$Ni molecular nanomagnets, Phys. Rev. B **90**, 184419 (2014).

[6] M. Shiddiq, D. Komijani, Y. Duan, A. Gaita-Ariño, E. Coronado, and S. Hill, Enhancing coherence in molecular spin qubits via atomic clock transitions, Nature **531**, 348 (2016).

[7] J. Ferrando-Soria, E. Moreno Pineda, A. Chiesa, A. Fernandez, S. A. Magee, S. Carretta, P. Santini, I. J. Vitorica-Yrezabal, F. Tuna, G. A. Timco, E. J. L. McInnes, and R. E. P. Winpenny, A modular design of molecular qubits to implement universal quantum gates, Nat. Commun. **7** (2016).

[8] C. Godfrin, A. Ferhat, R. Ballou, S. Klyatskaya, M. Ruben, W. Wernsdorfer, and F. Balestro, Operating quantum states in single magnetic molecules: Implementation of Grover's quantum algorithm, Phys. Rev. Lett. **119**, 187702 (2017).

[9] A. Gaita-Ariño, F. Luis, S. Hill, and E. Coronado, Molecular spins for quantum computation, Nature Chemistry **11**, 301 (2019).

[10] M. Atzori and R. Sessoli, The second quantum revolution: Role and challenges of molecular chemistry, J. Am. Chem. Soc. **141**, 11339 (2019).

[11] C. A. Collett, P. Santini, S. Carretta, and J. R. Friedman, Constructing clock-transition-based two-qubit gates from dimers of molecular nanomagnets, Phys. Rev. Research **2**, 032037 (2020).

[12] S. Carretta, D. Zueco, A. Chiesa, A. Gomez-Leon, and F. Luis, A perspective on scaling up quantum computation with molecular spins, Appl. Phys. Lett. **118**, 240501 (2021).

[13] F. Petiziol, A. Chiesa, S. Wimberger, P. Santini, and S. Carretta, Counteracting dephasing in molecular nanomagnets by optimized qudit encodings, npj Quantum Information **7**, 133 (2021).

[14] J. Liu, J. Mrozek, A. Ullah, Y. Duan, J. Baldoví, E. Coronado, A. Gaita-Ariño, and A. Ardavan, Quantum coherent spin–electric control in a molecular nanomagnet at clock transitions, Nature Physics **17**, 1205 (2021).

[15] A. Chiesa, F. Petiziol, M. Chizzini, P. Santini, and S. Carretta, Theoretical design of optimal molecular qudits for quantum error correction, J. Phys. Chem. Lett. **13**, 6468 (2022).

[16] G. Wolfowicz, A. M. Tyryshkin, R. E. George, H. Riemann, N. V. Abrosimov, P. Becker, H.-J. Pohl, M. L. W. Thewalt, S. A. Lyon, and J. J. L. Morton, Atomic clock transitions in silicon-based spin qubits, Nature Nanotechnol. **8**, 561 (2013).

[17] K. Kundu, J. R. K. White, S. A. Moehring, J. M. Yu, J. W. Ziller, F. Furche, W. J. Evans, and S. Hill, A 9.2-GHz clock transition in a Lu(II) molecular spin qubit arising from a 3.467-MHz hyperfine interaction, Nature Chem. **14**, 392 (2022).

[18] E. J. L. McInnes, Molecular spins clock in, Nature Chem. **14**, 361 (2022).

[19] K. Kundu, J. Chen, S. Hoffman, J. Marbey, D. Komijani, Y. Duan, A. Gaita-Ariño, X.-G. Zhang, H.-P. Cheng, and S. Hill, Demonstration of electron-nuclear decoupling at a spin clock transition, arXiv:2106.05185 (2021).

[20] P. Vorndamme and J. Schnack, Decoherence of a singlet-triplet superposition state under dipolar interactions of an uncorrelated environment, Phys. Rev. B **101**, 075101 (2020).

[21] Y. Bae, K. Yang, P. Willke, T. Choi, A. J. Heinrich, and C. P. Lutz, Enhanced quantum coherence in exchange coupled spins via singlet-triplet transitions, Science Advances **4**, eaau4159 (2018).

[22] J. Tang, I. Hewitt, N. T. Madhu, G. Chastanet, W. Wernsdorfer, C. E. Anson, C. Benelli, R. Sessoli, and A. K. Powell, Dysprosium triangles showing single-molecule magnet behavior of thermally excited spin states, Angew. Chem. Int. Ed. **45**, 1729 (2006).

[23] B. B. van Aken, J.-P. Rivera, H. Schmid, and M. Fiebig, Observation of ferrotoroidic domains, Nature **449**, 702 (2007).

[24] A. Soncini and L. F. Chibotaru, Toroidal magnetic states in molecular wheels: Interplay between isotropic exchange interactions and local magnetic anisotropy, Phys. Rev. B **77**, 220406 (2008).

[25] N. A. Spaldin, M. Fiebig, and M. Mostovoy, The toroidal moment in condensed-matter physics and its relation to the magnetoelectric effect, J. Phys.: Condens. Matter **20**, 434203 (2008).

[26] A. Soncini and L. F. Chibotaru, Molecular spintronics using noncollinear magnetic molecules, Phys. Rev. B **81**, 132403 (2010).

[27] P.-H. Guo, J.-L. Liu, Z.-M. Zhang, L. Ungur, L. F. Chibotaru, J.-D. Leng, F.-S. Guo, and M.-L. Tong, The first Dy_4 single-molecule magnet with a toroidal magnetic moment in the ground state, Inorg. Chem. **51**, 1233 (2012).

[28] L. Ungur, S. K. Langley, T. N. Hooper, B. Moubaraki, E. K. Brechin, K. S. Murray, and L. F. Chibotaru, Net toroidal magnetic moment in the ground state of a Dy_6-triethanolamine ring, J. Am. Chem. Soc. **134**, 18554 (2012).

[29] Y.-X. Wang, W. Shi, H. Li, Y. Song, L. Fang, Y. Lan, A. K. Powell, W. Wernsdorfer, L. Ungur, L. F. Chibotaru, M. Shen, and P. Cheng, A single-molecule magnet assembly exhibiting a dielectric transition at 470 k, Chem. Sci. **3**, 3366 (2012).

[30] S. Xue, X.-H. Chen, L. Zhao, Y.-N. Guo, and J. Tang, Two bulky-decorated triangular dysprosium aggregates conserving vortex-spin structure, Inorg. Chem. **51**, 13264 (2012).

[31] C. Das, S. Vaidya, T. Gupta, J. M. Frost, M. Righi, E. K. Brechin, M. Affronte, G. Rajaraman, and M. Shanmugam, Single-molecule magnetism, enhanced magnetocaloric effect, and toroidal magnetic moments in a family of Ln_4 squares, Chem. Eur. J. **21**, 15639 (2015).

[32] G. Fernandez Garcia, D. Guettas, V. Montigaud, P. Larini, R. Sessoli, F. Totti, O. Cador, G. Pilet, and B. Le Guennic, A Dy_4 cubane: A new member in the single-molecule toroics family, Angew. Chem. Int. Ed. **57**, 17089 (2018).

[33] K. R. Vignesh, S. K. Langley, A. Swain, B. Moubaraki, M. Damjanović, W. Wernsdorfer, G. Rajaraman, and K. S. Murray, Slow magnetic relaxation and single-molecule toroidal behaviour in a family of heptanuclear $Cr^{III}Ln_6^{III}$ (Ln=Tb, Ho, Er) complexes, Angew. Chem. Int. Ed. **57**, 779 (2018).

[34] J. M. Crabtree and A. Soncini, Toroidal quantum states in molecular spin-frustrated triangular nanomagnets with weak spin-orbit coupling: Applications to molecular spintronics, Phys. Rev. B **98**, 094417 (2018).

[35] S. K. Langley, K. R. Vignesh, T. Gupta, C. J. Gartshore, G. Rajaraman, C. M. Forsyth, and K. S. Murray, New examples of triangular terbium(III) and holmium(III) and hexagonal dysprosium(III) single molecule toroics, Dalton Trans. **48**, 15657 (2019).

[36] S. Rao, J. Ashtree, and A. Soncini, Toroidal moment in a family of spin-frustrated heterometallic triangular nanomagnets without spin-orbit coupling: Applications in a molecular spintronics device, Physica B **592**, 412237 (2020).

[37] Y. Pavlyukh, Toroidal spin states in molecular magnets, Phys. Rev. B **101**, 144408 (2020).

[38] H.-L. Zhang, Y.-Q. Zhai, L. Qin, L. Ungur, H. Nojiri, and Y.-Z. Zheng, Single-molecule toroic design through magnetic exchange coupling, Matter **2**, 1481 (2020).

[39] J. M. Ashtree, I. Borilovic, K. R. Vignesh, A. Swain, S. H. Hamilton, Y. L. Whyatt, S. L. Benjamin, W. Phonsri, C. M. Forsyth, W. Wernsdorfer, A. Soncini, G. Rajaraman, S. K. Langley, and K. S. Murray, Tuning the ferrotoroidic coupling and magnetic hysteresis in double-triangle complexes $\{Dy_3M^{III}Dy_3\}$ via the M^{III}-linker, Eur. J. Inorg. Chem. **5**, 435 (2021).

[40] K. Hymas and A. Soncini, The role of magnetic dipole-dipole coupling in quantum single-molecule toroics, Magnetochemistry **8**, 58 (2022).

[41] Q. Yang, L. Ungur, L. F. Chibotaru, and J. Tang, Toroidal versus centripetal arrangement of the magnetic moment in a Dy_4 tetrahedron, Chem. Commun. **58**, 1784 (2022).

[42] L. Chibotaru, L. Ungur, and A. Soncini, The origin of nonmagnetic kramers doublets in the ground state of dysprosium triangles: Evidence for a toroidal magnetic moment, Angew. Chem. Int. Ed. **47**, 4126 (2008).

[43] K. R. Vignesh, A. Soncini, S. K. Langley, W. Wernsdorfer, K. S. Murray, and G. Rajaraman, Ferrotoroidic ground state in a heterometallic $\{Cr^{III}Dy_6^{III}\}$ complex displaying slow magnetic relaxation, Nat. Commun. **8**, 1023 (2017).

[44] L. Ungur, S.-Y. Lin, J. Tang, and L. F. Chibotaru, Single-molecule toroics in ising-type lanthanide molecular clusters, Chem. Soc. Rev. **43**, 6894 (2014).

[45] F. Troiani, D. Stepanenko, and D. Loss, Hyperfine-induced decoherence in triangular spin-cluster qubits, Phys. Rev. B **86**, 161409 (2012).

[46] P. Vorndamme, H.-J. Schmidt, C. Schröder, and J. Schnack, Observation of phase synchronization and alignment during free induction decay of quantum spins with Heisenberg interactions, N. J. Phys. **23**, 083038 (2021).

[47] G. Lindblad, On the generators of quantum dynamical semigroups, Comm. Math. Phys. **48**, 119 (1976).

[48] F. Tabakin, Model dynamics for quantum computing, Annals of Physics **383**, 33 (2017).

[49] N. V. Prokof'ev and P. C. E. Stamp, Theory of the spin bath, Rep. Prog. Phys. **63**, 669 (2000).

[50] J. Chen, C. Hu, J. F. Stanton, S. Hill, H.-P. Cheng, and X.-G. Zhang, Decoherence in molecular electron spin qubits: Insights from quantum many-body simulations, J. Phys. Chem. Lett. **11**, 2074 (2020).

[51] E. R. Canarie, S. M. Jahn, and S. Stoll, Quantitative structure-based prediction of electron spin decoherence in organic radicals, J. Phys. Chem. Lett. **11**, 3396 (2020).

[52] M. Chizzini, L. Crippa, L. Zaccardi, E. Macaluso, S. Carretta, A. Chiesa, and P. Santini, Quantum error correction with molecular spin qudits, Phys. Chem. Chem. Phys. **24**, 20030 (2022).

[53] We speculate that superpositions of toroidal states can be obtained e.g. when molecules are deposited on surfaces using pulses of the STM tunneling current [55] or by microwave pulses in cases when the anisotropy axes are tilted from the molecular plane since the magnetization along the molecular axis is proportional to the toroidal moment of a given state.

[54] D. Pister, K. Irländer, D. Westerbeck, and J. Schnack, Toroidal magnetic molecules stripped to their basics, Phys. Rev. Research **4**, 033221 (2022).

[55] S. Baumann, W. Paul, T. Choi, C. P. Lutz, A. Ardavan, and A. J. Heinrich, Electron paramagnetic resonance of individual atoms on a surface, Science **350**, 417 (2015).